

## Article

# Genome-Wide Analysis of Tubulin Gene Family in Cassava and Expression of Family Member *FtsZ2-1* during Various Stress

Shuangbao Li <sup>1</sup>, Peng Cao <sup>1</sup>, Congcong Wang <sup>1</sup>, Jianchun Guo <sup>2</sup>, Yuwei Zang <sup>1</sup>, Kunlin Wu <sup>1</sup>, Fangfang Ran <sup>1</sup>, Liangwang Liu <sup>1</sup>, Dayong Wang <sup>1,\*</sup> and Yi Min <sup>1,\*</sup>

- <sup>1</sup> Department of Biosciences, School of Life and Pharmaceutical Sciences, Hainan University, Haikou 570228, China; 18071008210002@hainanu.edu.cn (S.L.); 17095103210001@hainanu.edu.cn (P.C.); wangcc2278655206@163.com (C.W.); 20071000110013@hainanu.edu.cn (Y.Z.); 19071001210008@hainanu.edu.cn (K.W.); 20071000210028@hainanu.edu.cn (F.R.); 20086000210026@hainanu.edu.cn (L.L.)
- <sup>2</sup> Institute of Tropical Bioscience and Biotechnology, Chinese Academy of Tropical Agricultural Sciences, Haikou 571101, China; guojianchun@itbb.org.cn
- \* Correspondence: wangdy@hainanu.edu.cn (D.W.); 992601@hainanu.edu.cn (Y.M.); Tel.: +86-187-8955-6728 (D.W.); +86-136-3761-6384 (Y.M.)

**Abstract:** Filamentous temperature-sensitive protein Z (Tubulin/*FtsZ*) family is a group of conserved GTP-binding (guanine nucleotide-binding) proteins, which are closely related to plant tissue development and organ formation as the major component of the cytoskeleton. According to the published genome sequence information of cassava (*Manihot esculenta* Crantz), 23 *tubulin* genes (*MeTubulins*) were identified, which were divided into four main groups based on their type and phylogenetic characteristics. The same grouping generally has the same or similar motif composition and exon–intron structure. Collinear analysis showed that fragment repetition event is the main factor in amplification of cassava *tubulin* superfamily gene. The expression profiles of *MeTubulin* genes in various tissue were analyzed, and it was found that *MeTubulins* were mainly expressed in leaf, petiole, and stem, while *FtsZ2-1* was highly expressed in storage root. The qRT-PCR results of the *FtsZ2-1* gene under hormone and abiotic stresses showed that indole-3-acetic acid (IAA) and gibberellin A3 (GA3) stresses could significantly increase the expression of the *FtsZ2-1* gene, thereby revealing the potential role of *FtsZ2-1* in IAA and GA3 stress-induced responses.

**Keywords:** cassava; tubulin; *FtsZ2-1*; duplication event; expression patterns; abiotic stress



**Citation:** Li, S.; Cao, P.; Wang, C.; Guo, J.; Zang, Y.; Wu, K.; Ran, F.; Liu, L.; Wang, D.; Min, Y. Genome-Wide Analysis of Tubulin Gene Family in Cassava and Expression of Family Member *FtsZ2-1* during Various Stress. *Plants* **2021**, *10*, 668. <https://doi.org/10.3390/plants10040668>

Academic Editor: Alex Troitsky

Received: 21 January 2021

Accepted: 28 March 2021

Published: 31 March 2021

**Publisher's Note:** MDPI stays neutral with regard to jurisdictional claims in published maps and institutional affiliations.



**Copyright:** © 2021 by the authors. Licensee MDPI, Basel, Switzerland. This article is an open access article distributed under the terms and conditions of the Creative Commons Attribution (CC BY) license (<https://creativecommons.org/licenses/by/4.0/>).

## 1. Introduction

Cell division is the process in which a cell is divided into two cells, which is the basis for the growth, development, and reproduction of organisms. Microtubules are polymerized by tubulins, which participate in cell division as one of the cytoskeleton systems, while tubulins are encoded by multiple gene families in plants [1,2]. The two most typical types of these gene families are  $\alpha$ -tubulin and  $\beta$ -tubulin, which account for more than 80% of the amount of tubulin, have similar three-dimensional structures, and can be closely combined into dimers as subunits of microtubule assembly [3–7]. In recent years,  $\gamma$ -tubulin has been discovered, which is located in the microtubule-organizing center and plays an important role in microtubule formation, number and location, polarity determination, and cell division [8–10]. These genes are specifically expressed in different tissues and organs, and their mutations may give rise to abnormal plant growth [11]. For instance, the decreased expression of  $\alpha$ -*tubulin6* (*TUA6*) gene led to abnormal shoot tip cell division and inhibited root elongation in *Arabidopsis thaliana* [12]. Transgenic rice plants with antisense expression of  $\beta$ -*tubulin8* (*OsTUB8*) were inhibited in the amount of seed set after ripening, and the height of plants was 20~60% lower than that of wild type [13].

*FtsZ*, homologs of tubulin, were first found in bacteria and involved in the bacterial division as cytoskeletal proteins, which became key proteins of chloroplast division in

higher plants with the occurrence of endosymbiotic events [14–19]. Generally, unlike bacteria just only one *FtsZ* gene, most plants contain three functionally complementary genes, *FtsZ1-1*, *FtsZ2-1*, and *FtsZ2-2*, which presumably arose by gene replication of a single ancestral *FtsZ* gene [20–25]. In plants, *FtsZ1-1* or *FtsZ2-1* null mutants can cause chloroplast division defects. Compared with the wild type, a decreased number and increased size of chloroplasts in the cell of green leaf were observed. Unlike *FtsZ1-1* and *FtsZ2-1* mutants, the phenotype of the *FtsZ2-2* null mutant is milder, and the number and size of the chloroplast are less variable [26,27]. During leaf growth, with the increase of chloroplasts in mesophyll cells to maximize photosynthesis, there is a negative correlation between chloroplast size and photosynthetic N-use efficiency (PNUE) [28,29].

The cytoskeleton tubulin and FtsZ proteins have similar functions; both are involved in polymer formation and play a key role in cell division, while tubulin and FtsZ proteins have little sequence identity but showed high conformational similarity [16,30]. Tubulin and FtsZ are GTPases, and their nucleotide-binding sites of tubulin and FtsZ are similar to those of GAPDH (glyceraldehyde-3-phosphate dehydrogenase) but different from nucleotide-binding sites of other typical GTPases [31,32]. Therefore, tubulin and FtsZ form a unique family of cytoskeletal GTPases [33]. Moreover, previous studies suggest that tubulin may have evolved from FtsZ at the beginning of eukaryotic evolution, which leads to extreme sequence divergence related to the shift in function [34].

Cassava is an important cash crop and food source growing in Africa, Asia, and tropical America because of its high starch content in storage root; about 750 million people depend on cassava as food [35,36]. Meanwhile, cassava can also be processed into flour, starch, animal feed, and alcohol [37]. It has strong tolerance and survival ability under biotic and abiotic stresses, and a relatively high yield under poor soil conditions [38]. This makes the production benefit of cassava significantly higher than other crops and more conducive to the rational allocation and utilization of land resources. Drought and salt are the main abiotic stresses affecting the growth of cassava [39]. In many coastal areas, the saline–alkali content in soil is often too high, causing harm to plants, while appropriate salt content can improve the nutritional level and starch content of cassava leaves. [40]. Spraying exogenous hormones can significantly affect the growth and development of cassava; for instance, a high concentration of MeJA could induce the cassava defense mechanism to play a role in advance [41–43]. The application of auxin can stimulate the growth of cassava stem and bud, and tubulins play an important role in this process [44–46]. Tubulins showed different responses under various stresses, such as high expression of soybean  $\beta$ -*tubulin1* gene under high concentration of auxin stress, while good stability under other abiotic stresses; the expression of  $\alpha$ -*tubulin2* gene from *Hevea brasiliensis* was regulated by NaCl, drought, and MeJA [47,48]. Based on the importance of the *tubulin* gene family during cassava growth, especially the regulation of FtsZ on chloroplast, it is of great significance to research the function of the cassava *tubulin* gene family to improve the quality of cassava. For this reason, we analyzed the gene characteristics, phylogeny, gene structure, gene repetition, protein motif, and expression profiles in various tissues, of cassava tubulin family members, and the expression of the *FtsZ2-1* gene was studied under IAA, MeJA, ABA, GA3, salt, and drought treatments.

## 2. Results

### 2.1. Identification of the Tubulin Proteins in Cassava

Through BLAST (basic local alignment search tool) search and HMMER (biosequence analysis using profile hidden Markov Models) analysis, 23 genes with tubulin domain were identified and annotated as MeTubulins in the cassava genome. According to the order of screening, 23 *MeTubulin* genes were named from *MeTubulin1* to *MeTubulin23*. Table 1, Tables S1 and S2 described information of the 23 *MeTubulins*, including gene ID, size, molecular weight (MW), isoelectric point (pI), and predicted subcellular location, chromosome number, the total number of positively and negatively charged residues, and sequence. *MeTubulin20* and *MeTubulin23* were identified as the smallest proteins,

both with 421 amino acids (aa), while the largest protein was MeTubulin10 (493 aa). In length with an average of 457 aa, the MW varied from 43.3 kDa (MeTubulin20) to 53.4 kDa (MeTubulin6), and the pI ranged from 4.68 (MeTubulin17) to 6.93 (MeTubulin20). The predicted subcellular localization indicated that MeTubulin10 and MeTubulin20 were positioned in chloroplast stroma, MeTubulin2 was shown to be localized in the chloroplast thylakoid membrane, and the rest of them were positioned in the cytoplasm.

**Table 1.** Information of 23 *MeTubulin* genes and proteins identified.

Gene Name	Gene ID	p-Value	Size (aa)	MW (KDa)	pI	Predicted Subcellular Location	Chr.
<i>MeTubulin1</i>	Manes.08G061700	$5.6 \times 10^{-114}$	454	50.31	4.76	cytoplasm	8
<i>MeTubulin2</i>	Manes.08G024800	$2.6 \times 10^{-43}$	492	51.13	5.56	chloroplast thylakoid membrane	8
<i>MeTubulin3</i>	Manes.02G136200	$3.4 \times 10^{-114}$	453	50.06	4.77	cytoplasm	2
<i>MeTubulin4</i>	Manes.02G123600	$2.8 \times 10^{-114}$	454	50.35	4.75	cytoplasm	2
<i>MeTubulin5</i>	Manes.05G200200	$2.7 \times 10^{-114}$	453	50.08	4.77	cytoplasm	5
<i>MeTubulin6</i>	Manes.05G025900	$6 \times 10^{-94}$	481	53.40	5.70	cytoplasm	5
<i>MeTubulin7</i>	Manes.05G147000	$1.5 \times 10^{-112}$	456	50.38	4.74	cytoplasm	5
<i>MeTubulin8</i>	Manes.13G106300	$8.6 \times 10^{-94}$	424	45.79	4.93	cytoplasm	13
<i>MeTubulin9</i>	Manes.09G100400	$2.2 \times 10^{-113}$	451	49.93	4.85	cytoplasm	9
<i>MeTubulin10</i>	Manes.09G055800	$1.6 \times 10^{-42}$	493	51.31	5.96	chloroplast stroma	9
<i>MeTubulin11</i>	Manes.09G140200	$1.5 \times 10^{-98}$	456	49.69	5.00	cytoplasm	9
<i>MeTubulin12</i>	Manes.06G058600	$8 \times 10^{-112}$	451	49.89	4.78	cytoplasm	6
<i>MeTubulin13</i>	Manes.06G007200	$2 \times 10^{-114}$	454	50.39	4.72	cytoplasm	6
<i>MeTubulin14</i>	Manes.06G147900	$9 \times 10^{-115}$	454	50.33	4.75	cytoplasm	6
<i>MeTubulin15</i>	Manes.15G108500	$3.3 \times 10^{-99}$	456	49.70	5.00	cytoplasm	15
<i>MeTubulin16</i>	Manes.01G249000	$7.2 \times 10^{-94}$	480	53.24	5.67	cytoplasm	1
<i>MeTubulin17</i>	Manes.01G061400	$4.2 \times 10^{-112}$	453	50.12	4.68	cytoplasm	1
<i>MeTubulin18</i>	Manes.01G166100	$2.6 \times 10^{-114}$	454	50.35	4.74	cytoplasm	1
<i>MeTubulin19</i>	Manes.14G124600	$1.1 \times 10^{-113}$	451	49.84	4.78	cytoplasm	14
<i>MeTubulin20</i>	Manes.03G135500	$6.1 \times 10^{-38}$	421	43.29	6.93	chloroplast stroma	3
<i>MeTubulin21</i>	Manes.03G098100	$2.8 \times 10^{-100}$	457	49.74	4.90	cytoplasm	3
<i>MeTubulin22</i>	Manes.10G087300	$3.7 \times 10^{-100}$	457	49.57	4.93	cytoplasm	10
<i>MeTubulin23</i>	Manes.10G087200	$3.8 \times 10^{-73}$	421	45.61	4.74	cytoplasm	10

## 2.2. Multiple Sequence Alignment, Phylogenetic Analysis, and Classification of MeTubulins

As shown in Figure 1, using the tubulin protein sequences of cassava, *Oryza sativa*, *Hevea brasiliensis*, *Arabidopsis thaliana*, *Dioscorea rotundata*, and *Vitis vinifera*, the unrooted phylogenetic trees were constructed by the maximum likelihood (ML) method, and their evolutionary relationship were further analyzed. A total of 115 tubulins contained 31 *Hevea brasiliensis*, 16 *Arabidopsis thaliana*, 16 *Oryza sativa Japonica*, 11 *Dioscorea rotundata*, and 18 *Vitis vinifera*, which were divided into groups I, II, III, and IV corresponding to  $\beta$ -tubulin,  $\alpha$ -tubulin,  $\gamma$ -tubulin and FtsZ based on the four types of tubulin (Table S3). In addition, referring to the classification of Radchuk et al. [49], group I can be divided into three subgroups, Ia to Ic, and group II can be divided into two subgroups, IIa and IIb. Group Ia consisted of 22 tubulins, usually containing two introns, including five MeTubulins (MeTubulin7, 12, 13, 17, and 19), together with six HbTubulins from *Hevea brasiliensis*, four AtTubulins from *Arabidopsis thaliana*, four OsTubulins from *Oryza sativa Japonica*, three VitTubulins from *Vitis vinifera*, and one DrTubulin from *Dioscorea rotundata*. Three MeTubulins (MeTubulin1, 3, and 5), one AtTubulin, three VitTubulins, three OsTubulin10, two HbTubulins, and one DrTubulins belonged to group Ib, which generally contains an extra intron in the 5' untranslated region. Group Ic mainly consisted of dicotyledons, four MeTubulins (MeTubulin4, 9, 14, and 18), two AtTubulins, seven HbTubulins, and three ViTubulins, and only two monocotyledons OsTubulin10, and DrTubulin2. Similarly, group IIa usually contains three introns, including three MeTubulins (MeTubulin8, 22,

and 23), together with two AtTubulins, four HbTubulins, two OsTubulins, four VitTubulins, and two DrTubulins. Group IIIb generally contains four introns, consisting of three MeTubulins (MeTubulin11, 15, and 21), two AtTubulins, two VitTubulins, two OsTubulins, four HbTubulins, and two DrTubulins. Two MeTubulins (MeTubulin 6 and 16) clustered with two AtTubulins, DrTubulin7, three HbTubulins, OsTubulin4, and VitTubulin13 in group III. Group IV consisted of three MeTubulins (MeTubulin 2, 10, and 20), three AtTubulins, three DrTubulins, three OsTubulins, two VitTubulins, and three HbTubulins. HbTubulin4 was excluded from the grouping because it was too divergent. Furthermore, a total of four sister pairs of MeTubulins were showed in the phylogenetic tree, including MeTubulin2–MeTubulin10, MeTubulin8–MeTubulin23, MeTubulin15–MeTubulin21, MeTubulin12–MeTubulin19. Tubulin domain sequence alignment of MeTubulin proteins showed that sequence varied greatly from position 33 to 46 amino acids, but the sequence was identical or similar in the same group (Figure 2).

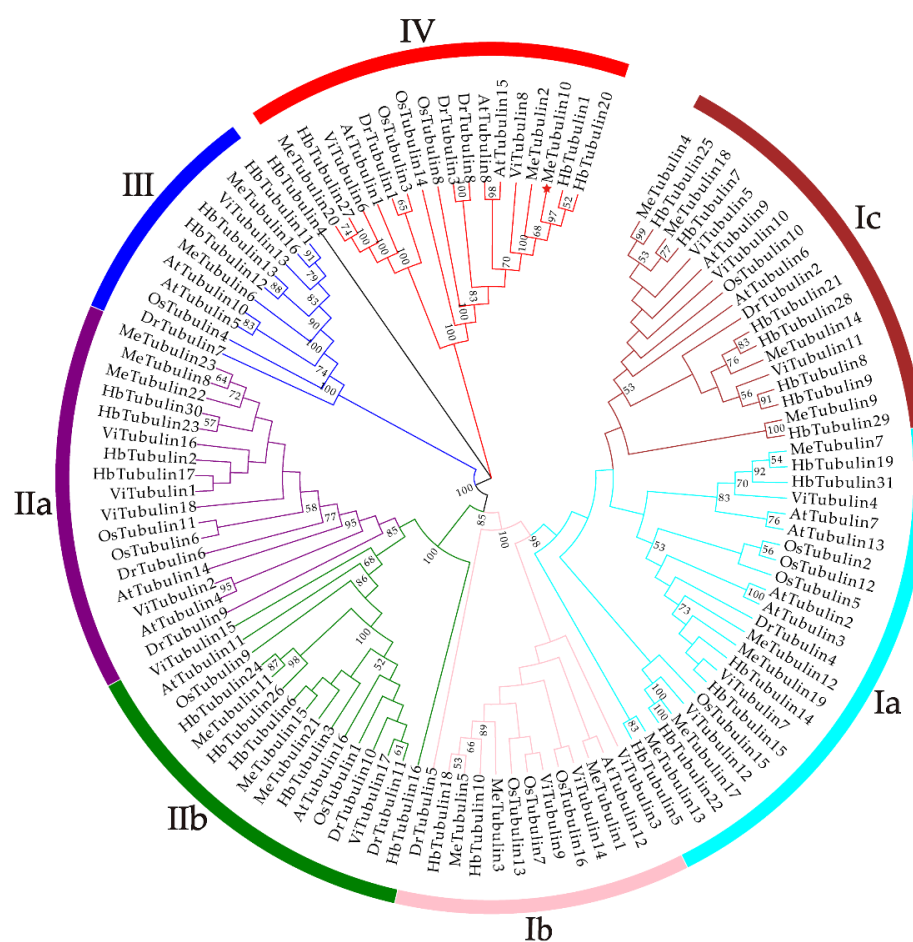


**Figure 1.** The phylogenetic tree represents the relationship between tubulin proteins in six species. The bootstrap values of less than 50% were hidden. The different-colored arcs and roman numerals indicate different groups (or subgroups) of tubulin proteins. The red star (MeTubulin10) represent FtsZ2-1 from cassava. The branch length values are shown in Supplementary Figure S1.





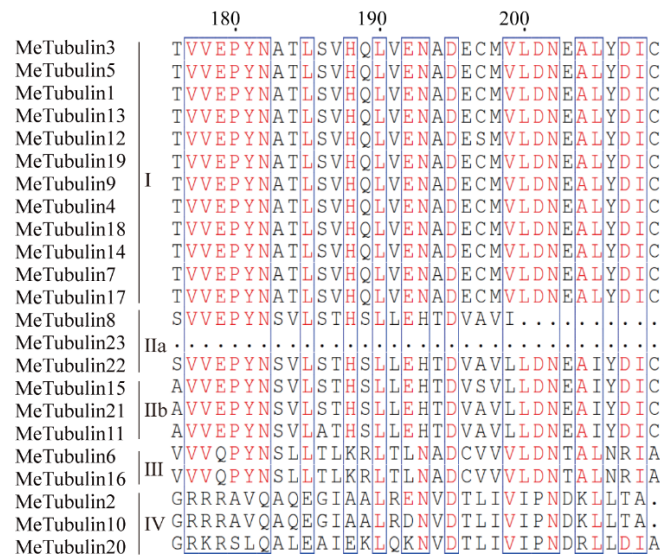


**Figure 2.** Tubulin domain sequence alignment of MeTubulin proteins. Dots represent gaps, blue frames represent the conserved region, red columns indicate the identical residues, and red letters indicate conserved residues.

### 2.3. Gene Structure and Motif Composition of MeTubulins

For this study, 10 conserved motifs of MeTubulins with a length of 20 amino acids were identified by the MEME program; the function of these motifs have not been clarified (Table S4). As exhibited in Figure 3A,B, it was found that MeTubulins with similar motif composition tend to be clustered together. For instance, groups I and II contain all motifs (except for Metubulin23), group III mainly lacks motifs 3, 7, and 2, and group IV only shares a common motif 9.

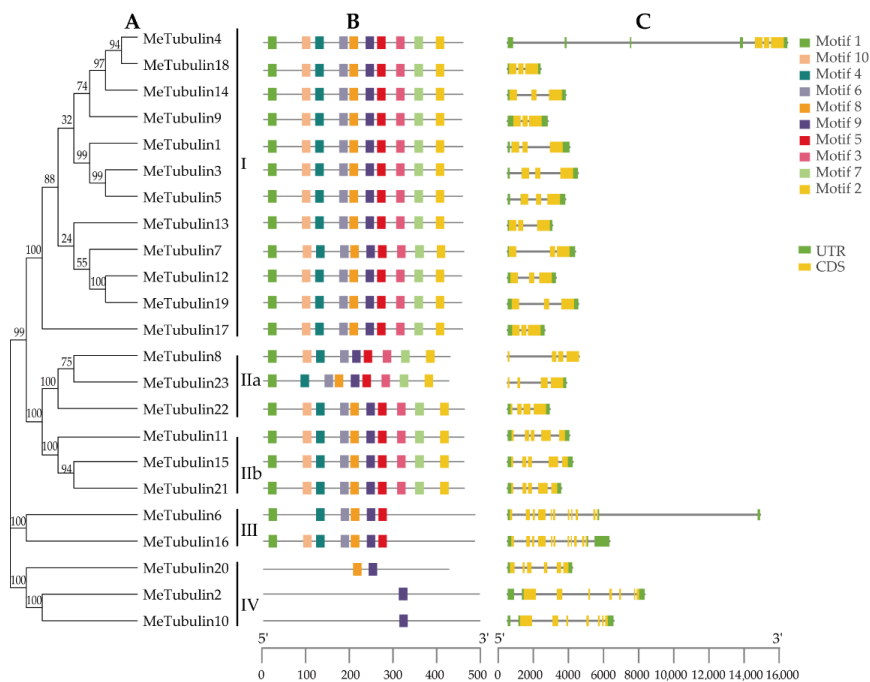


**Figure 3.** Phylogenetic relationships, gene structure, and conserved motifs in *tubulin* genes from cassava. (A) The phylogenetic tree was constructed according to the full-length sequences of cassava tubulin using MEGA 7.0. (B) The motif composition of cassava tubulin. The motifs (numbers 1–10) are represented by rectangles of different colors. Supplementary Table S4 contains the amino acid sequence, E-value, and functional annotation of each motif. (C) Exon–intron organization of *MeTubulins*. Green rectangles represent untranslated 5'- and 3'-regions; yellow rectangle represents coding sequences (CDS); introns are represented by black lines. The scale at the bottom is to estimate the length of the protein.

In order to gain a better understanding of the evolution of the cassava tubulin family, the exon–intron structures of all identified *MeTubulin* genes were analyzed. All *MeTubulin* genes displayed 3 to 11 exons (12 with 3 exons, 3 with 4 exons, 3 with 5 exons, 1 with 6 exons, 2 with 7 exons, and 2 with 11 exons) in Figure 3C. Significantly, each group has the same number of exons (except for the IV group, two contain seven exons and one contains six exons). Meanwhile, the number of introns in the same group is also similar. Generally, the diversity of exon–intron structure makes the gene family show a variety of different functions and could be used as a basis for phylogenetic grouping.

#### 2.4. Chromosome Distribution and Synteny Analysis of *MeTubulins* Gene

In total, 23 *MeTubulins* were unevenly distributed on 11 chromosomes, and each chromosome contained 1–3 *MeTubulins* in Supplementary Figure S2. A total of 11 segmental duplication genes were obtained from 23 *MeTubulins* by BLASTP and multiple collinearity scan toolkit (MCScanX) methods in Figure 4 (Table S5). The results show that these *MeTubulin* genes might be produced by segmental replication events.

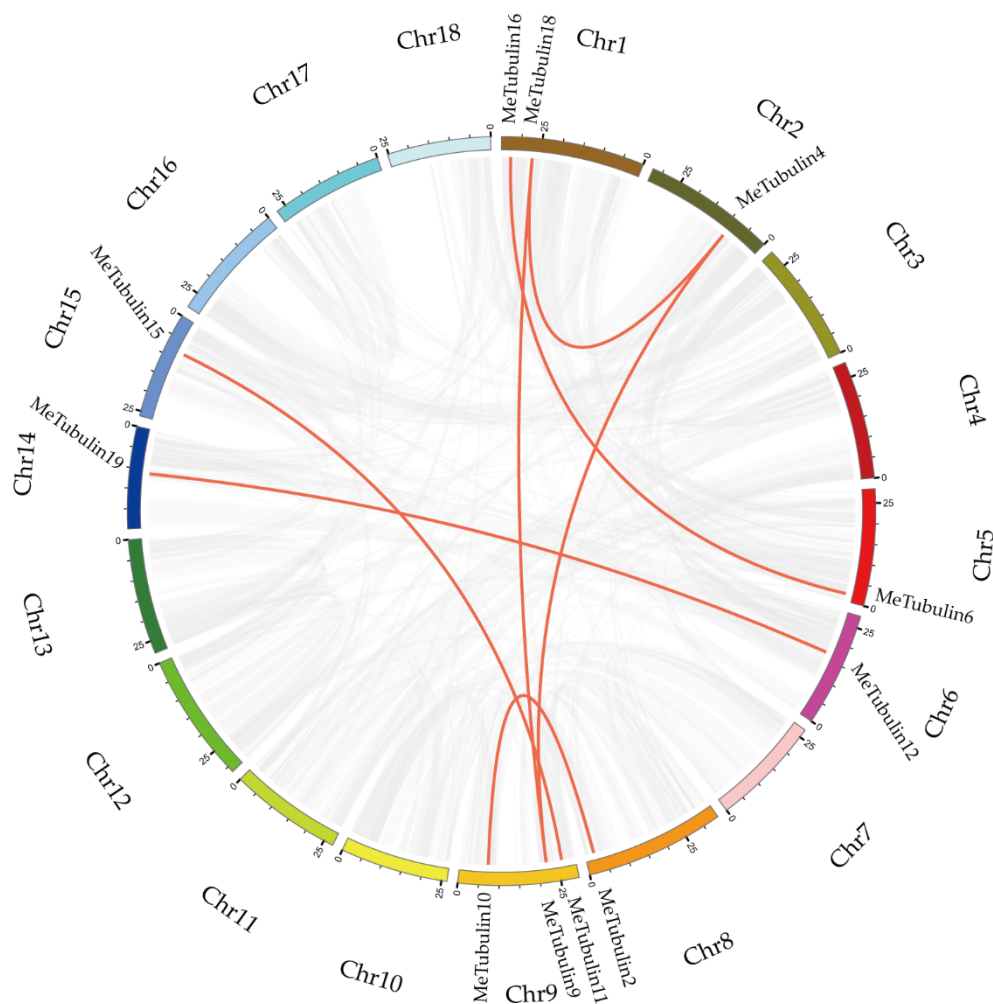


**Figure 4.** Schematic representations for the chromosomal distribution and inter-chromosomal relationships of *MeTubulins*. The synteny blocks in the cassava genome are represented by gray lines, and the duplicated *tubulin* gene pairs are by red lines. The bottom of each chromosome shows the chromosome number.

To research the evolutionary mechanisms of the cassava *tubulin* family further, five comparative syntenic maps of cassava associated with five representative species were constructed, including two monocots (*Oryza sativa* and *Dioscorea rotundata*) and three dicots (*Populus trichocarpa*, *Arabidopsis thaliana*, and *Vitis vinifera*) (Figure 5). In general, cassava



and dicotyledons have more collinear genes than monocotyledons (Table S6). For example, *Dioscorea rotundata* (7), and *Oryza sativa* (1) have fewer collinear genes than *Vitis vinifera* (18), *Populus trichocarpa* (14), and *Arabidopsis thaliana* (9). Some MeTubulins have been observed to be associated with more than one syntenic gene pairs, especially cassava and *Vitis vinifera*, such as MeTubulin9 and MeTubulin17, speculated that these genes might play a significant role in the evolution of the MeTubulin family.



**Figure 5.** Synteny analysis of *tubulin* genes between cassava and five representative plant species. Gray lines in the background represent the collinear blocks within cassava and other plant genomes, while the red lines highlight the syntenic *tubulin* gene pairs. The species names with the prefixes ‘*M. esculenta*’, ‘*A. thaliana*’, ‘*D. rotundata*’, ‘*P. trichocarpa*’, ‘*O. sativa*’ and ‘*V. vinifera*’ indicate *Manihot esculenta*, *Arabidopsis thaliana*, *Dioscorea rotundata*, *Populus trichocarpa*, *Oryza sativa*, and *Vitis vinifera*, respectively.



### 2.5. Expression Profiles of *MeTubulins* in Different Tissue Types

The RNA-seq data publicly available from the GEO (gene expression omnibus) database under the accession number GSE7951 [50], which contained expression profiling (Table S8) of 11 cassava tissue types (root apical meristem (RAM), leaf, petiole, stem, midvein, lateral bud, storage root, fibrous root, stem apical meristem (SAM), in addition to organized embryogenic structures (OES) and friable embryogenic callus (FEC) for genome editing and transgene integration) were used in expression analysis of cassava *Tubulin* genes (Figure 6). We found that some *MeTubulins* have similar expressions in the same tissue. *MeTubulin1*, *MeTubulin3*, *MeTubulin4*, *MeTubulin5*, *MeTubulin6*, *MeTubulin10*, *MeTubulin17*, *MeTubulin19*, *MeTubulin22*, and *MeTubulin23* showed high levels of expression in petioles and stems, of which *MeTubulin10* was also highly expressed in storage root. *MeTubulin2*, *MeTubulin7*, *MeTubulin9*, *MeTubulin11*, *MeTubulin12*, *MeTubulin13*, *MeTubulin15*, *MeTubulin20*, and *MeTubulin21* were highly expressed in leaves and midveins, *MeTubulin14*, *MeTubulin16*, and *MeTubulin18* exhibited high expression levels FEC and SAM, and *MeTubulin8* exhibited higher expression levels in RAM and storage roots.

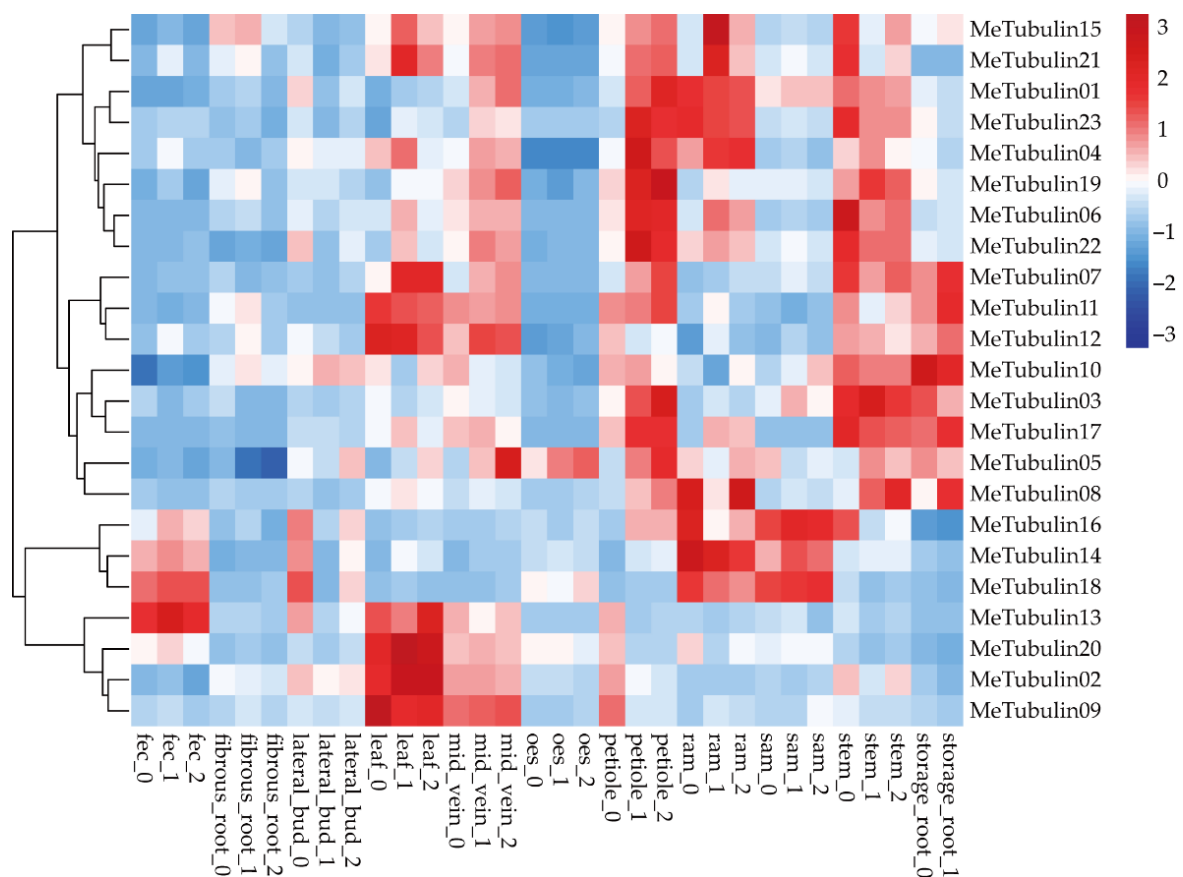


**Figure 6.** Expression profiles of the cassava *tubulin* genes. Hierarchical clustering of expression profiles of cassava *tubulin* genes in various tissue types.

### 2.6. Expression Patterns of *FtsZ2-1* Gene in Response to Various Stresses

Cassava seedlings were treated with IAA, MeJA (methyl jasmonate), ABA (abscisic acid), GA3, NaCl, and PEG (polyethylene glycol) treatments to research the expression of the *FtsZ2-1* gene by different abiotic stresses and hormonal treatments (Figure 7). Under 100  $\mu$ M IAA treatment, the expression of *FtsZ2-1* fluctuated with time. The expression of *FtsZ2-1* increased at the beginning, then decreased and subsequently increased again, reached the peak at 8 h, and decreased sharply at 12 h. After that, the expression level approached the peak at 48 h. After treatment with 100  $\mu$ M MeJA, the expression of *FtsZ2-1*

fluctuated with time; it decreased significantly after treatment, reaching the lowest value at 4 h, and then increased to the highest value at 24 h. Under 100  $\mu$ M GA3 treatment, the expression of *FtsZ2-1* showed an upward trend with the delay of time, decreased at 8 h, and then continued to rise for 48 h to reach the peak. Under the abiotic stress of 300 mM NaCl and 20% PEG, the transcriptional level of *FtsZ2-1* decreased at first and then increased. The difference was that the expression level of *FtsZ2-1* reached the lowest level at 4 h and reached the highest level at 48 h after the treatment with 300 mM NaCl, which was significantly higher than that in the control group. However, under 20% PEG treatment, the transcriptional level decreased rapidly to the lowest level at 2 h and increased to a similar level as that of the control group at 48 h.

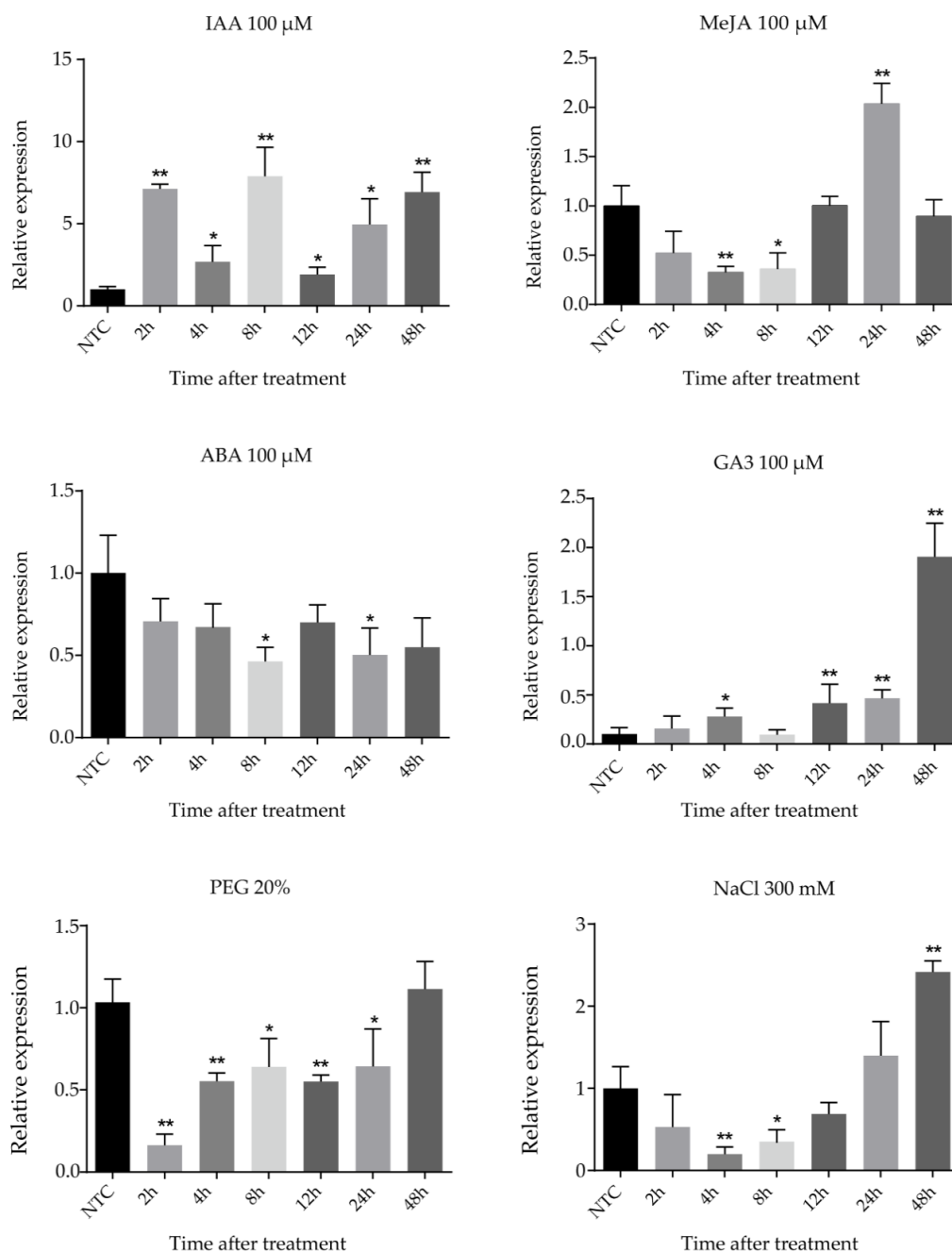


**Figure 7.** Expression profiles of *FtsZ2-1* gene in response to various stress treatments. Data were normalized to the *tubulin* gene and vertical bars indicate standard deviation. Asterisk (\*) significant and \*\* highly significant) denote significant variation ( $p < 0.05$ ).

### 3. Discussion

Tubulins consist of cytoskeleton proteins that are present in all plant species. Understanding the role of tubulins in growth and non-specific response to abiotic stress factors in plants is essential [6,51]. In our study, the phylogenetic tree, genetic structure, gene replication protein motif, and expression profiles in different tissues of the tubulin family in cassava were analyzed. Furthermore, the expression of the *FtsZ2-1* gene under various stresses was researched. Tubulin genes were screened from the cassava genome, along with six other species, for instance, *Arabidopsis thaliana* [52], *Dioscorea rotundata* [53], *Hevea brasiliensis* [54], *Oryza sativa* [55], and *Vitis vinifera* [56]. In this study, 23 cassava tubulins were found and renamed as *MeTubulin1* to *MeTubulin23* in the order of screening, lower than *Hevea brasiliensis* (31), but higher than *Arabidopsis thaliana* (16), *Dioscorea rotundata* (11), *Oryza sativa* (16), and *Vitis vinifera* (18); according to amino acid sequences, motif composition, intron structure, phylogenetic feature, and tubulin type of cassava, the 23 cassava tubulin genes can be divided into four main groups.

Multiple sequence comparisons were used to analyze the conserved domains of cassava tubulins. The results showed that *MeTubulin23* had the least conserved residues, and *MeTubulin2*, *MeTubulin10*, and *MeTubulin23* had low similarity with other amino acid sequences (Table S7). The gain and loss of domain is the diverging force of gene family members' diversity. The sequence variation of domains is relatively common in rice and maize [57–59]. Thus, the function and binding specificity of specified four tubulin proteins deserve further study.

The phylogenetic tree divides tubulin proteins into four main groups, and each group contains only one tubulin type from cassava, *Vitis vinifera*, *Oryza sativa*, *Hevea brasiliensis*, *Dioscorea rotundata*, and *Arabidopsis thaliana*, and the neighboring tubulins in the same group might have similar functions; for instance, *HbTubulin27*, *VitTubulin6*, *AtTubulin1*, and *OsTubulin3* are involved in the regulation of plastid division [27,60–62]. Overall, 10 conserved motifs were identified in the cassava tubulin family, and it was found that members with similar motif composition had cognate gene structures and were clustered together on the phylogenetic tree. This indicates that the tubulin family is evolutionarily diverse and conservative.

In the course of evolution, gene diversity proceeds through sequence divergence, recombination, and replication [63]. Gene replication events have been often considered important sources of evolutionary dynamics [64]. Tandem duplication and segmental replication lead to the expansion of gene families [65]. Based on the explanation of Holub, tandem duplication of a gene is a chromosomal region within 200 kb containing two or more genes [66]. In the *MeTubulin* family, seven pairs of genes were found to be derived from fragment repeat evolution, but no tandem repeat was found, which means that the driving force of the family expansion is mainly fragment repeat (Figure 4). Purification selection was the main driving force for differentiation of *MeTubulin* replication based on  $K_a/K_s$  values below 1 (Table S8) [67]. The *FtsZ2-1* gene in cassava has fragment duplication and a colinear relationship with corresponding genes in dicotyledons (*Arabidopsis thaliana* and *Vitis vinifera*) and monocotyledon (*Dioscorea rotundata*).

The expression profiles of *MeTubulin* in various tissues were analyzed by using RNA-seq (RNA sequencing) data of cassava in the GEO database, which is helpful to research the potential function of the *MeTubulin* gene (Figure 7), and several *MeTubulins* showed tissue-specific expression in specific tissues. For instance, *MeTubulin2*, *MeTubulin10*, and *MeTubulin20* are highly expressed in leaf, and they are involved in the formation of chloroplast in mesophyll cell, which is similar to the homologous genes *AtTubulin8*, *AtTubulin15*, and *AtTubulin1* in *Arabidopsis thaliana* [68,69]. Hence, highly expressed genes might play a role in the physiological process of corresponding tissues, which provides a new idea for researching the potential function of *MeTubulin* genes in cassava.

To date, accumulated pieces of evidence show that plant hormones and abiotic stress play a crucial role in the growth and development of cassava [70,71]. *FtsZ2-1*, a member of the tubulin family, was selected for different stress treatments, and its function was

further explored through the transcriptional response to different treatments in our research. IAA, which may be produced by the terminal buds, limits water transport to the lateral buds, and the change of water movement alters the composition of membrane lipids, thus inducing the growth of lateral buds [72]. Exogenous MeJA could delay cell deterioration, maintain postharvest longevity, reduce cell oxidative damage, and regulate storage quality by activating superoxide dismutase, catalase, and peroxidase [70]. In addition, it can induce plant chemical defense by stimulating the expression of plant defense genes [73]. ABA plays a regulatory role in plant growth and under the influence of the external environment [74]. The application of ABA, through foreign aid, can accelerate the adaptation of some crops to cold and drought [75,76]. Furthermore, it was found that GA3 affected the synthesis of cassava starch by regulating the activities of key enzymes in the process of starch synthesis [77]. It was noteworthy that the expression pattern of the *FtsZ2-1* gene is not completely consistent with that of previous studies, which may be caused by the inhibition of growth by a high concentration of IAA and the promotion of growth at low concentration, indicating that *FtsZ2-1* is closely related to the growth of cassava. [67]. The expression of *FtsZ2-1* changed significantly under MeJA treatment, which provides a new idea for studying the functional mechanism of MeJA in cassava. However, there was little difference in the expression of *FtsZ2-1* under ABA treatment, which indicated that *FtsZ2-1* may not be an important factor affecting the mechanism of action of ABA. The level of *FtsZ2-1* transcripts increased significantly after GA3 treatment, indicating that *FtsZ2-1* might be an important member involved in the regulation mechanism of GA3. The main abiotic environmental stresses are salt and drought stresses. Solving water shortage and salt stress is a global problem to ensure the survival of agricultural crops and sustainable metabolism of food production [78]. The expression trends of the *FtsZ2-1* gene induced by PEG and NaCl were similar, which provides an opportunity to study the relationship between drought and salt action mechanism. From these results, the *FtsZ2-1* gene might play a role in cassava growth and environmental stress.

#### 4. Materials and Methods

##### 4.1. Identification of the Tubulin Gene Family

The whole genome sequence of cassava was downloaded from the EnsemblPlant database ([http://plants.ensembl.org/Manihot\\_esculenta/Info/Index](http://plants.ensembl.org/Manihot_esculenta/Info/Index), access date: 22 June 2020). Local BLAST searches were performed based on the hidden Markov model (HMM) profile of tubulin domains from the Pfam database under the accession number PF00091 (<http://pfam.xfam.org/family/PF00091#tabview=tab6>, access date: 1 July 2020) [43,79]. The selected tubulin protein sequence was submitted to the CDD (conserved domain database) website (<https://www.ncbi.nlm.nih.gov/cdd/>, access date: 12 July 2020) and SMART website (<http://smart.embl.de/>, access date: 8 July 2020) with default parameters to confirm the conservative tubulin domain [80]. The sequence length, MW, pI, and subcellular location prediction of cassava tubulin proteins were obtained by online ExPASy (<http://web.expasy.org/protparam/>, access date: 5 August 2020) and Psort server (<http://psort1.hgc.jp/form.html>, access date: 1 August 2020) with default parameters.

##### 4.2. Sequence Analysis and Structural Characterization

The gene structures were analyzed by the gene structure display server (GSDS: <http://gsds.cbi.pku.edu.cn>, access date: 21 August 2020) [81]. The structure of exon/intron was determined by comparing genomic DNA and CDS sequences of tubulin genes. The MEME online program (<http://meme.nbcr.net/meme/intro.html>, access date: 20 September 2020) was used to analyze the conserved motifs in full-length tubulin proteins, with the following parameters: the site distribution, any number of repetitions; the number of motifs, 10; optimum motif length = 10–20 residues, and shuffle the sequences several times under the same parameters to ensure the reliability of motif [82]. Meanwhile, all identified motifs were annotated according to InterProScan (<http://www.ebi.ac.uk/Tools/pfa/iprscan/>, access date: 8 March 2021).



#### 4.3. Chromosomal Localization and Gene Duplication

The location of *MeTubulin* genes on the chromosome was analyzed by MapChart software (<https://www.wur.nl/en/show/Mapchart.htm>, access date: 20 October 2020) [83]. Multiple collinearity scan toolkit (MCScanX) was used to analyze the gene duplication events, and the parameters were the default values [84]. The synthetic map of each tubulin gene duplicated segment was generated by CIRCOS software (<http://circos.ca/>, access date: 20 October 2020) [85]. The putative duplicated genes were linked by connection lines. The syntenic analysis maps were constructed by using our own coded python program to prove the homologous relationship of orthologous Tubulin genes obtained from cassava and other selected species [86]. Non-synonymous (ka) and synonymous (ks) substitution of each duplicated tubulin genes were calculated using KaKs\_Calculator 2.0 (<https://sourceforge.net/projects/kakscalculator2/>, access date: 18 November 2020) [87].

#### 4.4. Phylogenetic Analysis of Cassava Tubulin Genes Family

The whole protein sequences of MeTubulin, AtTubulin, HbTubulin, ViTubulin, DrTubulin, and OsTubulin were according to the descriptions in the relevant literature and obtained from the EnsemblPlant database (<http://plants.ensembl.org/>, access date: 22 June 2020). All tubulin proteins were compared by ClustalW [88]. The maximum likelihood (ML) phylogenetic tree based on the full length of protein sequences was constructed by using MEGA 7.0, with the following preferences (Analysis: Phylogeny Reconstruction; Statistical Method: Maximum Likelihood; Test of Phylogeny: Bootstrap method; No. of Bootstrap Replications: 1000; Substitutions Type: Amino acid; Model/Method: Poisson model; Site Coverage Cutoff (%): 50; ML Heuristic Method: Nearest-Neighbor-Interchange (NNI); Initial Tree for ML: Make initial tree automatically (Default-NJ/BioNJ); Branch Swap Filter: Moderate) [89,90].

#### 4.5. RNA-Seq Data Analysis of Tubulin Genes

The RNA-seq data of cassava (Table S9) were obtained from the GEO database (<https://www.ncbi.nlm.nih.gov/geo/query/acc.cgi?acc=GSE82279> access date: 22 October 2020) to research the expression profiles of *tubulin* genes in different tissue types. Based on Hiplot tool (<https://hiplot.com.cn/basic/heatmap> access date: 15 February 2021), the absolute FPKM (Fragments per kilobase of exon per million fragments mapped) values were divided by the average of all values, and the ratios were transformed by log<sub>2</sub> to obtain data that are suitable for cluster displays, and the heatmap was generated [91].

#### 4.6. Plant Materials and Treatments

SC8 (South China 8), a typical cassava cultivar was derived from the Tropical Crops Genetic Resource Institute (TCGRI, Danzhou, China). A large number of plants regenerated from tissue culture were obtained by using lateral buds of cassava on MS medium. Then, they were transferred to soil culture for two months to select seedlings with similar growth status for subsequent experiments. To study the expression pattern of the *FtsZ2-1* gene under different abiotic stresses and hormone treatments, further qRT-PCR analysis was carried out. For hormone treatments, cassava seedlings were sprayed with 100 µM IAA, MeJA, ABA, and GA3, respectively, and the leaves were collected at 2, 4, 8, 12, 24, and 48 h after treatment. In addition, 300 mM NaCl and 20%PEG were used to simulate salt stress and drought stress, which were consistent with the way of hormone treatments. All treated leaves were immediately frozen in liquid nitrogen and stored at −80 °C for subsequent analysis.

#### 4.7. RNA Extraction and qRT-PCR Analysis

The RNA of each sample was extracted according to Trizol Reagent (Invitrogen #15596026). All RNA was analyzed by 1% agarose gel electrophoresis and then quantified with a Nanodrop ND-1000 spectrophotometer. RNA was used for the synthesis of the first strand of cDNA by using HiScript<sup>®</sup> III SuperMix for qPCR (+ gDNA wiper) Kit (Vazyme

#R323) according to the manufacturer's recommendations. ChamQ™ Universal SYBR® qPCR Master Mix (Vazyme #Q711) was used for qRT-PCR on a Roche Lightcycler® 480. The reaction system is as follows: 5.0 µL 2 × ChamQ Universal SYBR® qPCR Master Mix, 0.2 µL forward primers, 0.2 µL reverse primers, 1.0 µL template cDNA, 3.6 µL ddH<sub>2</sub>O. The PCR reaction was carried out under the following condition: preincubation (95 °C for 60 s), 40 cycles of three-step amplification (95 °C for 10 s, 60 °C for 15 s, and 72 °C for 15 s), melting (95 °C for 10 s, 65 °C for 15 s, and 97 °C for 1 s), and cooling (37 °C for 30 s). According to the related literature, the cassava *β-tubulin* gene (*MeTubulin1*) was suitable to be used as an internal reference for all the qRT-PCR analyses [92]. The specific primers were designed on the basis of *β-tubulin* and *FtsZ2-1* (*MeTubulin10*) CDS sequences (Table S2) by Primer 5.0 software (*β-tubulin*-F: GTTATCCCCTTCCTCCCTCGTCT, *β-tubulin*-R: TCCTTGGTGCTCATCTCTTCC3 and *FtsZ2-1*-F: GCCATCCTCATCATTACCGA, *FtsZ2-1*-R: TGGACATCCTAGCAAAGCAGA). Each sample was performed with three independent replications. Relative expression levels were calculated by the  $2^{-\Delta\Delta C_t}$  method [93]. The expression of the *FtsZ2-1* gene at each time point was compared to the corresponding NTC (no treatment control). Statistical differences were analyzed by one-way ANOVA, followed by the post hoc tests, and a *p*-value less than 0.05 was deemed as significant. The data were processed and plotted in pictures by the GraphPad Prism 7.0.

## 5. Conclusions

In the study, a genome-wide analysis of the tubulin family in cassava was carried out, and 23 *MeTubulin* genes were identified. The biochemical characteristics of proteins, prediction of subcellular localization, gene structure, conservative motifs, chromosome location, and gene replication were analyzed, and their basic classification and evolutionary characteristics were established. This biological information provides plentiful resources for the functional identification of *tubulin* genes. The expression atlas analysis of the *MeTubulin* genes provides evidence of the potential functions of these genes in specific tissues. Moreover, analysis of *FtsZ2-1* gene expression under different treatments showed that the *FtsZ2-1* gene had a comprehensive response to IAA, MeJA, ABA, NaCl, and PEG. In general, this study laid a foundation for further analysis of the function of the *MeTubulin* gene family.

**Supplementary Materials:** The following are available online at <https://www.mdpi.com/article/10.3390/plants10040668/s1>, Figure S1: the phylogenetic tree represents the relationship between tubulin proteins in six species, and show the branch length values, Figure S2: genome-wide distribution and orientation of *MeTubulin* genes on cassava chromosomes. Table S1, S2: list of the 23 *MeTubulin* genes and proteins identified in this study, Table S3: list of the 124 *tubulin* genes in the phylogenetic tree, Table S4: analysis and distribution of conserved motifs and in cassava tubulin proteins, Table S5: segmentally duplicated *MeTubulin* gene pairs, Table S6: one-to-one orthologous relationships between cassava and other five plant species, Table S7: information of the 23 tubulin domains, Table S8: orthologous relationships between cassava, Table S9: RNA-seq data of 23 *MeTubulin* genes that were used in this study.

**Author Contributions:** Conceptualization, S.L. and Y.M.; software, S.L. and P.C.; resources, Y.M.; data curation, S.L. and C.W.; writing—original draft preparation, S.L. and D.W.; writing—review and editing, S.L., Y.Z., K.W., J.G., F.R., and L.L.; project administration, S.L.; funding acquisition, Y.M.; All authors have read and agreed to the published version of the manuscript.

**Funding:** This research was supported by the National Natural Science Foundation of China (No.31960039); Hainan Provincial Natural Science Foundation of China (319MS007); Central Public-interest Scientific Institution Basal Research Fund for Chinese Academy of Tropical Agricultural Sciences (No.1630052020009, 1630052020010); The Earmarked Fund for China Agriculture Research System (CARS-11-HNGJC).

**Conflicts of Interest:** The authors declare that they have no conflict of interests.

## References

1. Steven, R.; Ludwig, D.G. Characterization of the  $\alpha$ -tubulin gene family of *Arabidopsis thaliana*. *Genetics* **1987**, *84*, 5833–5837.
2. Sutkovic, J.; Gawwad, M.R. In silico prediction of three-dimensional structure and interactome analysis of Tubulin  $\alpha$  subfamily of *Arabidopsis thaliana*.pdf. *Netw. Biol.* **2014**, *4*, 47–57.
3. Gavazzi, F.; Pigna, G.; Braglia, L.; Giani, S.; Breviario, D.; Morello, L. Evolutionary characterization and transcript profiling of beta-tubulin genes in flax (*Linum usitatissimum* L.) during plant development. *BMC Plant Biol.* **2017**, *17*, 237. [[CrossRef](#)]
4. Lowe, J.; Li, H.; Downing, K.H.; Nogales, E. Refined structure of  $\alpha\beta$ -tubulin at 3.5 resolution 1. *J. Mol. Biol.* **2001**, *313*, 1045–1057. [[CrossRef](#)] [[PubMed](#)]
5. Serna, M.; Carranza, G.; Martín-Benito, J.; Janowski, R.; Canals, A.; Coll, M.; Zabala, J.C.; Valpuesta, J.M. The structure of the complex between  $\alpha$ -tubulin, TBCE and TBCB reveals a tubulin dimer dissociation mechanism. *J. Cell Sci.* **2015**, *128*, 1824–1834. [[CrossRef](#)]
6. Oakley, R.V.; Wang, Y.S.; Ramakrishna, W.; Harding, S.A.; Tsai, C.J. Differential expansion and expression of alpha- and beta-tubulin gene families in *Populus*. *Plant Physiol.* **2007**, *145*, 961–973. [[CrossRef](#)] [[PubMed](#)]
7. Pydiura, N.; Pirko, Y.; Galinowsky, D.; Postovoitova, A.; Yemets, A.; Kilchevsky, A.; Blume, Y. Genome-wide identification, phylogenetic classification, and exon-intron structure characterization of the tubulin and actin genes in flax (*Linum usitatissimum*). *Cell Biol. Int.* **2019**, *43*, 1010–1019. [[CrossRef](#)] [[PubMed](#)]
8. Dryková, D.; Cenklová, V.; Sulimenko, V.; Volc, J.; Dráber, P.; Binarová, P. Plant  $\gamma$ -tubulin interacts with  $\alpha\beta$ -tubulin dimers and forms membrane-associated complexes. *Plant Cell* **2003**, *15*, 465–480. [[CrossRef](#)] [[PubMed](#)]
9. Kállai, B.M.; Kourová, H.; Chumová, J.; Papdi, C.; Binarová, P.  $\gamma$ -Tubulin interacts with E2FA, E2FB and E2FC transcription factors, regulates proliferation and endocycle in *Arabidopsis*. *J. Exp. Bot.* **2019**, *71*, 498–531. [[CrossRef](#)]
10. Miao, H.; Guo, R.; Chen, J.; Wang, Q.; Lee, Y.J.; Liu, B. The gamma-tubulin complex protein GCP6 is crucial for spindle morphogenesis but not essential for microtubule reorganization in *Arabidopsis*. *Proc. Natl. Acad. Sci. USA* **2019**, *116*, 27115–27123. [[CrossRef](#)]
11. Silflow, C.D.; Oppenheimer, D.G.; Kopozak, S.D.; Ploense, S.E.; Ludwig, S.R.; Haas, N.; Snustad, D.P. Plant tubulin genes structure and differential expression during development. *Genetics* **1987**, *8*, 435–460. [[CrossRef](#)]
12. Bao, Y.; Kost, B.; Chua, N.H. Reduced expression of  $\alpha$ -tubulin genes in *Arabidopsis thaliana* specifically affects root growth and morphology, root hair development and root gravitropism. *Plant J.* **2001**, *28*, 145–157. [[CrossRef](#)] [[PubMed](#)]
13. Yang, G.; Jan, A.; Komatsu, S. Functional analysis of OsTUB8, an anther-specific  $\beta$ -tubulin in rice. *Plant Sci.* **2007**, *172*, 832–838. [[CrossRef](#)]
14. Du, S.; Lutkenhaus, J. Assembly and activation of the *Escherichia coli* divisome. *Mol. Microbiol.* **2017**, *105*, 177–187. [[CrossRef](#)] [[PubMed](#)]
15. Erickson, H.P.; Anderson, D.E.; Osawa, M. FtsZ in bacterial cytokinesis: Cytoskeleton and force generator all in one. *Microbiol. Mol. Biol. Rev.* **2010**, *74*, 504–528. [[CrossRef](#)] [[PubMed](#)]
16. Lwe, J.; Amos, L.A. Crystal structure of the bacterial cell-division protein FtsZ. *Nature* **1998**, *391*, 203–206. [[CrossRef](#)]
17. Ma, X.; Ehrhardt, D.W.; Margolin, W. Colocalization of cell division proteins FtsZ and FtsA to cytoskeletal structures in living *Escherichia coli* cells by using greenfluorescentprotein. *Proc. Natl. Acad. Sci. USA* **1996**, *93*, 12998–13003. [[CrossRef](#)]
18. Miyagishima, S.Y.; Takahara, M.; Mori, T.; Kuroiwa, H.; Kuroiwa, H.T. Plastid division is driven by a complex mechanism that involves differential transition of the bacterial and eukaryotic division rings. *Plant Cell* **2001**, *13*, 2257–2268. [[CrossRef](#)]
19. Stanislav Vitha, R.S.; Katherine, W.O. FtsZ ring formation at the chloroplast division site in plants. *J. Cell Biol.* **2001**, *153*, 111–120. [[CrossRef](#)]
20. Chen, C.; Maccready, J.S.; Ducat, D.C.; Osteryoung, K.W. The molecular machinery of chloroplast division. *Plant Physiol.* **2018**, *176*, 138–151. [[CrossRef](#)]
21. Grosche, C.; Rensing, S.A. Three rings for the evolution of plastid shape: A tale of land plant FtsZ. *Protoplasma* **2017**, *254*, 1879–1885. [[CrossRef](#)]
22. Osteryoung, K.W.; Vierling, E. Conserved cell and organelle division. *Nature* **1995**, *376*, 473–474. [[CrossRef](#)]
23. Terbush, A.D.; Yoshida, Y.; Osteryoung, K.W. FtsZ in chloroplast division: Structure, function and evolution. *Curr. Opin. Cell Biol.* **2013**, *25*, 461–470. [[CrossRef](#)]
24. Osteryoung, K.W.; Stokes, K.D.; Rutherford, S.M.; Percival, A.L.; Lee, W.Y. Chloroplast division in higher plants requires members of two functionally divergent gene families with homology to bacterial ftsZ. *Plant Cell* **1998**, *10*, 1991–2004. [[CrossRef](#)] [[PubMed](#)]
25. Schmitz, A.J.; Glynn, J.M.; Olson, B.J.; Stokes, K.D.; Osteryoung, K.W. *Arabidopsis* FtsZ2-1 and FtsZ2-2 are functionally redundant, but FtsZ-based plastid division is not essential for chloroplast partitioning or plant growth and development. *Mol. Plant* **2009**, *2*, 1211–1222. [[CrossRef](#)] [[PubMed](#)]
26. McAndrew, R.S.; Olson, B.J.; Kadirjan-Kalbach, D.K.; Chi-Ham, C.L.; Vitha, S.; Froehlich, J.E.; Osteryoung, K.W. In vivo quantitative relationship between plastid division proteins FtsZ1 and FtsZ2 and identification of ARC6 and ARC3 in a native FtsZ complex. *Biochem. J.* **2008**, *412*, 367–378. [[CrossRef](#)] [[PubMed](#)]
27. Yoder, D.W.; Kadirjan-Kalbach, D.; Olson, B.J.; Miyagishima, S.Y.; Deblasio, S.L.; Hangarter, R.P.; Osteryoung, K.W. Effects of mutations in *Arabidopsis* FtsZ1 on plastid division, FtsZ ring formation and positioning, and FtsZ filament morphology in vivo. *Plant Cell Physiol.* **2007**, *48*, 775–791. [[CrossRef](#)] [[PubMed](#)]

28. Leech, R.M.; Baker, N.R. Growth and functioning of leaves. In *Development of Photosynthetic Capacity in Leaves, Proceedings of the 13th International Botanical Congress, University of Sydney, Sydney, Australia, 18–20 August 1981*; Cambridge University Press: Cambridge, UK, 1983.
29. Yong, L.; Binbin, R.; Lei, D.; Qirong, S.; Shaobing, P.; Shiwei, G.; Ive, D.S. Does chloroplast size influence photosynthetic nitrogen Use efficiency. *PLoS ONE* **2013**, *8*, e62036.
30. Nogales, E.; Wolf, S.G.; Downing, K.H. Structure of the alpha beta tubulin dimer by electron crystallography. *Nature* **1998**, *391*, 199–203. [[CrossRef](#)]
31. Nogales, E.; Downing, K.H.; Amos, L.A.; Lowe, J. Tubulin and FtsZ form a distinct family of GTPases. *Nat. Struct. Mol. Biol.* **1998**, *5*, 451–458. [[CrossRef](#)]
32. Carlier, M.F.; Pantaloni, D. Kinetic analysis of guanosine 5'-triphosphate hydrolysis associated with tubulin polymerization. *Biochemistry* **1981**, *20*, 1918–1924. [[CrossRef](#)] [[PubMed](#)]
33. Krol, E.; de Sousa Borges, A.; da Silva, I.; Polaquini, C.R.; Regasini, L.O.; Ferreira, H.; Scheffers, D.J. Antibacterial activity of alkyl gallates is a combination of direct targeting of FtsZ and permeabilization of bacterial membranes. *Front. Microbiol.* **2015**, *6*, 390–401. [[CrossRef](#)] [[PubMed](#)]
34. Yutin, N.; Koonin, E.V. Archaeal origin of tubulin. *Biol. Direct* **2012**, *7*, 10–18. [[CrossRef](#)] [[PubMed](#)]
35. Dufour, D.L. Cyanide content of cassava (*Manihot esculenta*, Euphorbiaceae) cultivars used by tukanoan indians in northwest amazonia. *Econ. Bot.* **1988**, *42*, 255–266. [[CrossRef](#)]
36. Westby, A.; Hillocks, R.J.; Thresh, J.M. Cassava utilization, storage and small-scale processing. *Cassava Biol. Prod. Util.* **2002**, *14*, 281–300.
37. Jiao, J.; Li, J.; Bai, Y. Uncertainty analysis in the life cycle assessment of cassava ethanol in China. *J. Clean. Prod.* **2019**, *206*, 438–451. [[CrossRef](#)]
38. Okogbenin, E.; Setter, T.L.; Ferguson, M.; Mutege, R.; Ceballos, H.; Olasanmi, B.; Fregene, M. Phenotypic approaches to drought in cassava: Review. *Front. Physiol.* **2013**, *4*, 93–105. [[CrossRef](#)] [[PubMed](#)]
39. Cheng, Y.E.; Dong, M.Y.; Fan, X.W.; Nong, L.L.; Li, Y.Z. A study on cassava tolerance to and growth responses under salt stress. *Environ. Exp. Bot.* **2018**, *155*, 429–440. [[CrossRef](#)]
40. Gleadow, R.; Pegg, A.; Blomstedt, C.K. Resilience of cassava (*Manihot esculenta* Crantz) to salinity: Implications for food security in low-lying regions. *J. Exp. Bot.* **2016**, *67*, 5403–5413. [[CrossRef](#)] [[PubMed](#)]
41. Cao, P.; Liu, X.; Guo, J.; Chen, Y.; Li, S.; Wang, C.; Huang, W.; Min, Y. Genome-wide analysis of Dynamin gene family in cassava (*Manihot esculenta* Crantz) and transcriptional regulation of family members ARC5 in hormonal treatments. *Int. J. Mol. Sci.* **2019**, *20*, 5094. [[CrossRef](#)]
42. Wei, Y.; Shi, H.; Xia, Z.; Tie, W.; Ding, Z.; Yan, Y.; Wang, W.; Hu, W.; Li, K. Genome-wide identification and expression Analysis of the WRKY gene family in cassava. *Front. Plant Sci.* **2016**, *7*, 25–42. [[CrossRef](#)]
43. Rauwane, M.; Ntushelo, K. Understanding biotic stress and hormone signalling in cassava (*Manihot esculenta*): Potential for using hyphenated analytical techniques. *Appl. Sci.* **2020**, *10*, 8152. [[CrossRef](#)]
44. Blume, Y.B.; Krasnylenko, Y.A.; Yemets, A.I. Effects of phytohormones on the cytoskeleton of the plant cell. *Russ. J. Plant Physiol.* **2012**, *59*, 515–529. [[CrossRef](#)]
45. Fan, S.; Chang, Y.; Liu, G.; Shang, S.; Tian, L.; Shi, H. Molecular functional analysis of auxin/indole-3-acetic acid proteins (Aux/IAAs) in plant disease resistance in cassava. *Physiol. Plant.* **2020**, *168*, 88–97. [[CrossRef](#)]
46. Li, K.; Zhu, W.; Zeng, K.; Zhang, Z.; Ye, J.; Ou, W.; Rehman, S.; Heuer, B.; Chen, S. Proteome characterization of cassava (*Manihot esculenta* Crantz) somatic embryos, plantlets and tuberous roots. *Proteome Sci.* **2010**, *8*, 10–21. [[CrossRef](#)] [[PubMed](#)]
47. Lee, E.A.; Jo, H.Y.; Han, I.S. Auxin activates promoter of a soybean  $\beta$ -tubulin, tubB1 gene. *Korean J. Genet.* **2005**, *27*, 383–388.
48. Yang, H.; Deng, Z.; Liu, H.; Dai, L.J.; Li, D.J. Cloning, expression and bioinformatics analysis of HbTUA2 gene in *Hevea brasiliensis* (rubber tree). *Plant Physiol. J.* **2017**, *53*, 52–62.
49. Radchuk, V.V. The transcriptome of the tubulin gene family in plants. In *The Plant Cytoskeleton: A Key Tool for Agro-Biotechnology*; Springer: Dordrecht, The Netherlands, 2009; pp. 219–241.
50. Wilson, M.C.; Mutka, A.M.; Hummel, A.W.; Berry, J.; Chauhan, R.D.; Vijayaraghavan, A.; Taylor, N.J.; Voytas, D.F.; Chitwood, D.H.; Bart, R.S. Gene expression atlas for the food security crop cassava. *New Phytol.* **2017**, *213*, 1632–1641. [[CrossRef](#)]
51. Baranova, E.N.; Christov, N.K.; Kurenina, L.V.; Khaliluev, M.R.; Todorovska, E.G.; Smirnova, E.A. Formation of atypical tubulin structures in plant cells as a nonspecific response to abiotic stress. *Bulg. J. Agric. Sci.* **2016**, *22*, 987–992.
52. Alonso, J.M.; Stepanova, A.N.; Lisse, T.J.; Kim, C.J.; Chen, H.; Shinn, P.; Stevenson, D.K.; Zimmerman, J.; Barajas, P.; Cheuk, R.; et al. Genome-wide insertional mutagenesis of *Arabidopsis thaliana*. *Science* **2003**, *301*, 653–657. [[CrossRef](#)]
53. Zhang, Y.M.; Chen, M.; Sun, L.; Wang, Y.; Yin, J.; Liu, J.; Sun, X.Q.; Hang, Y.Y. Genome-wide identification and evolutionary analysis of NBS-LRR genes from *Dioscorea rotundata*. *Front. Genet.* **2020**, *11*, 484–494. [[CrossRef](#)]
54. Li, H.L.; Guo, D.; Yang, Z.P.; Tang, X.; Peng, S.Q. Genome-wide identification and characterization of WRKY gene family in *Hevea brasiliensis*. *Genomics* **2014**, *104*, 14–23. [[CrossRef](#)] [[PubMed](#)]
55. Jain, M.; Tyagi, A.K.; Khurana, J.P. Genome-wide analysis, evolutionary expansion, and expression of early auxin-responsive SAUR gene family in rice (*Oryza sativa*). *Genomics* **2006**, *88*, 360–371. [[CrossRef](#)] [[PubMed](#)]
56. Cheng, C.; Wang, Y.; Chai, F.; Li, S.; Xin, H.; Liang, Z. Genome-wide identification and characterization of the 14-3-3 family in *Vitis vinifera* L. during berry development and cold- and heat-stress response. *BMC Genom.* **2018**, *19*, 579–592. [[CrossRef](#)]



57. Brand, L.H.; Fischer, N.M.; Harter, K.; Kohlbacher, O.; Wanke, D. Elucidating the evolutionary conserved DNA-binding specificities of WRKY transcription factors by molecular dynamics and in vitro binding assays. *Nucleic Acids Res.* **2013**, *41*, 9764–9778. [[CrossRef](#)] [[PubMed](#)]
58. Fiume, E.; Christou, P.; Gian, S.; Breviario, D. Introns are key regulatory elements of rice tubulin expression. *Planta* **2004**, *218*, 693–703. [[CrossRef](#)] [[PubMed](#)]
59. Wei, K.F.; Chen, J.; Chen, Y.F.; Wu, L.J.; Xie, D.X. Molecular phylogenetic and expression analysis of the complete WRKY transcription factor family in maize. *DNA Res.* **2012**, *19*, 153–164. [[CrossRef](#)]
60. Kawagoe, Y. Septum Formation in Amyloplasts Produces Compound Granules in the Rice Endosperm and is Regulated by Plastid Division Proteins. *Plant Cell Physiol.* **2010**, *51*, 1469–1479.
61. Tangphatsornruang, S.; Uthaipaisanwong, P.; Sangsrakru, D.; Chanprasert, J.; Yoocha, T.; Jomchai, N.; Tragoonrung, S. Characterization of the complete chloroplast genome of *Hevea brasiliensis* reveals genome rearrangement, RNA editing sites and phylogenetic relationships. *Gene* **2011**, *475*, 104–112. [[CrossRef](#)]
62. Xianyun, M.U.; Shen, X.; Yuanmi, W.U.; Zhu, Y.; Dong, S.; Xia, X.; Lin, Q.; Fan, P.; Liu, Y.; Zhang, Z. Plastid phylogenomic study of grape species and its implications for evolutionary study and conservation of *Vitis*. *Phytotaxa* **2018**, *364*, 71–80.
63. Chothia, C.; Gough, J.; Vogel, C.; Teichmann, S.A. Evolution of the protein repertoire. *Science* **2003**, *300*, 1701–1703. [[CrossRef](#)]
64. Ohno, S.; Wolf, U.; Atkin, N.B. Evolution from fish to mammals by gene duplication. *Hereditas* **1968**, *59*, 169–187. [[CrossRef](#)]
65. Cannon, S.B.; Mitra, A.; Baumgarten, A.; Young, N.D.; May, G. The roles of segmental and tandem gene duplication in the evolution of large gene families in *Arabidopsis thaliana*. *BMC Plant Biol.* **2004**, *4*, 10–30. [[CrossRef](#)]
66. Holub, E.B. The arms race is ancient history in *Arabidopsis*, the wildflower. *Nat. Rev. Genet.* **2001**, *2*, 516–527. [[CrossRef](#)]
67. Zhang, Z.; Li, J.; Zhao, X.Q.; Wang, J.; Wong, K.S.; Yu, J. KaKs\_Calculator: Calculating Ka and Ks through model selection and model averaging. *Genom. Proteom. Bioinform.* **2006**, *4*, 259–263. [[CrossRef](#)]
68. Geng, M.T.; Min, Y.; Yao, Y.; Chen, X.; Fan, J.; Yuan, S.; Wang, L.; Sun, C.; Zhang, F.; Shang, L.; et al. Isolation and characterization of *ftsZ* genes in cassava. *Genes* **2017**, *8*, 391. [[CrossRef](#)]
69. Kadirjan-Kalbach, D.K.; Turmo, A.; Wang, J.; Smith, B.C.; Chen, C.; Porter, K.J.; Childs, K.L.; DellaPenna, D.; Osteryoung, K.W. Allelic variation in the chloroplast division gene *FtsZ2-2* leads to natural variation in chloroplast size. *Plant Physiol.* **2019**, *181*, 1059–1074. [[CrossRef](#)]
70. Hu, W.; Yang, H.; Yan, Y.; Wei, Y.; Tie, W.; Ding, Z.; Zuo, J.; Peng, M.; Li, K. Genome-wide characterization and analysis of bZIP transcription factor gene family related to abiotic stress in cassava. *Sci. Rep.* **2016**, *6*, 22783–22794. [[CrossRef](#)]
71. Sojikul, P.; Saithong, T.; Kalapanulak, S.; Pisuttinustart, N.; Limsirichaikul, S.; Tanaka, M.; Utsumi, Y.; Sakurai, T.; Seki, M.; Narangajavana, J. Genome-wide analysis reveals phytohormone action during cassava storage root initiation. *Plant Mol. Biol.* **2015**, *88*, 531–543. [[CrossRef](#)]
72. Wang, S.Y.; Faust, M.; Line, M.J. Apical dominance in apple (*malus domestica* borkh): The possible role of indole-3-acetic acid (IAA). *Sci. Hortic.* **1994**, *60*, 167–172. [[CrossRef](#)]
73. Bertini, L.; Proietti, S.; Focaracci, F.; Sabatini, B.; Caruso, C. Epigenetic control of defense genes following MeJA-induced priming in rice (*O. sativa*). *J. Plant Physiol.* **2018**, *228*, 166–177.
74. Zhao, H.; Wu, C.; Yan, Y.; Tie, W.; Ding, Z.; Liu, G.; Yan, W.; Li, Y.; Wang, W.; Peng, M.; et al. Genomic analysis of the core components of ABA signaling reveals their possible role in abiotic stress response in cassava. *Environ. Exp. Bot.* **2019**, *167*, 103855. [[CrossRef](#)]
75. Quarrie, S.A. Genotypic differences in leaf water potential, abscisic acid and proline concentrations in spring wheat during drought stress. *Ann. Bot.* **1980**, *46*, 383–394. [[CrossRef](#)]
76. Schaffer, M.A.; Fischer, R.L. Analysis of mRNAs that accumulate in response to low temperature identifies a thiol protease gene in tomato. *Plant Physiol.* **1988**, *87*, 431–436. [[CrossRef](#)] [[PubMed](#)]
77. Heng-Rui, L.I.; Jian-Kun, Z.; Wen-Wu, Q.; Lian-Jun, L.; Chong, P.; Zhen-Hua, L.; Qiu-Lian, N.; Jia-Wen, L.; Zhou-Mei, M.O.; Mei-Ying, L.U. Relationship between endogenous gibberellin and starch accumulation in cassava tuber. *Hubei Agric. Sci.* **2015**, *54*, 1628–1632.
78. Kang, M.S. *Water and Agricultural Sustainability Strategies*; CRC Press: Leiden, The Netherlands; Balkema: Leiden, The Netherlands, 2010; pp. 169–278.
79. Potter, S.C.; Aurelien, L.; Eddy, S.R.; Youngmi, P.; Rodrigo, L.; Finn, R.D. HMMER web server: 2018 update. *Nucleic Acids Res.* **2018**, *46*, W200–W204. [[CrossRef](#)]
80. Zhao, P.; Wang, D.; Wang, R.; Kong, N.; Zhang, C.; Yang, C.; Wu, W.; Ma, H.; Chen, Q. Genome-wide analysis of the potato Hsp20 gene family: Identification, genomic organization and expression profiles in response to heat stress. *BMC Genom.* **2018**, *19*, 61–73. [[CrossRef](#)]
81. Guo, A.Y.; Zhu, Q.H.; Chen, X.; Luo, J.C. GSDB: A gene structure display server. *Hereditas* **2007**, *29*, 1023–1026. [[CrossRef](#)]
82. Tao, P.; Zhong, X.; Li, B.; Wang, W.; Yue, Z.; Lei, J.; Guo, W.; Huang, X. Genome-wide identification and characterization of aquaporin genes (AQPs) in Chinese cabbage (*Brassica rapa* ssp. *pekinensis*). *Mol. Genet. Genom.* **2014**, *289*, 1131–1145. [[CrossRef](#)]
83. Voorrips, R.E. MapChart: Software for the graphical presentation of linkage maps and QTLs. *Hered* **2002**, *93*, 77–78. [[CrossRef](#)]
84. Wang, Y.; Tang, H.; Debarry, J.D.; Tan, X.; Li, J.; Wang, X.; Lee, T.H.; Jin, H.; Marler, B.; Guo, H.; et al. MCScanX: A toolkit for detection and evolutionary analysis of gene synteny and collinearity. *Nucleic Acids Res.* **2012**, *40*, e49. [[CrossRef](#)] [[PubMed](#)]

85. Krzywinski, M.; Schein, J.; Birol, I.; Connors, J.; Gascoyne, R.; Horsman, D.; Jones, S.J.; Marra, M.A. Circos: An information aesthetic for comparative genomics. *Genome Res.* **2009**, *19*, 1639–1645. [[CrossRef](#)] [[PubMed](#)]
86. Liu, C.; Xie, T.; Chen, C.; Luan, A.; Long, J.; Li, C.; Ding, Y.; He, Y. Genome-wide organization and expression profiling of the R2R3-MYB transcription factor family in pineapple (*Ananas comosus*). *BMC Genom.* **2017**, *18*, 503–518. [[CrossRef](#)] [[PubMed](#)]
87. Wang, D.; Zhang, Y.; Zhang, Z.; Zhu, J.; Yu, J. KaKs\_Calculator 2.0: A toolkit Incorporating gamma-series methods and sliding window Strategies. *Genom. Proteom. Bioinform.* **2010**, *8*, 77–80. [[CrossRef](#)]
88. Larkin, M.A.; Blackshields, G.; Brown, N.P.; Chenna, R.M.; Mcgettigan, P.A.; Mcwilliam, H.; Valentin, F.; Wallace, I.M.W.; Wilm, A.; Lopez, R.; et al. Clustal X version 2.0. *Bioinformatics* **2007**, *23*, 2947–2948. [[CrossRef](#)]
89. Kumar, S.; Stecher, G.; Tamura, K. MEGA7: Molecular evolutionary genetics analysis version 7.0 for bigger datasets. *Mol. Biol. Evol.* **2016**, *33*, 1807–1817. [[CrossRef](#)]
90. Chuang, K.S.; Jan, M.L.; Wu, J.; Lu, J.C.; Chen, S.; Hsu, C.H.; Fu, Y.K. A maximum likelihood expectation maximization algorithm with thresholding. *Comput. Med. Imaging Graph.* **2005**, *29*, 571–578. [[CrossRef](#)]
91. Howe, E.A.; Sinha, R.; Schlauch, D.; Quackenbush, J. RNA-Seq analysis in MeV. *Bioinformatics* **2011**, *27*, 3209–3210. [[CrossRef](#)]
92. Salcedo, A.; Zambrana, C.; Siritunga, D. Comparative expression analysis of reference genes in field-grown cassava. *Trop. Plant Biol.* **2014**, *7*, 53–64. [[CrossRef](#)]
93. Schmittgen, T.D.; Livak, K.J. Analyzing real-time PCR data by the comparative CT method. *Nat. Protoc.* **2008**, *3*, 1101–1108. [[CrossRef](#)]